Supplementary Information

Biochar Boost: Revolutionizing Functionalization of a Difficult Material

Sara M. K. Cheema – *Department of Chemistry, Memorial University of Newfoundland, St. John's, Newfoundland and Labrador A1B 3X7, Canada*

Celine M. Schneider – *Department of Chemistry, Memorial University of Newfoundland, St. John's, Newfoundland and Labrador A1B 3X7, Canada*

Pascale Chevallier – *Laboratory for Biomaterials and Bioengineering (LBB-UL), Department of Min-Met-Materials Engineering & Division Regenerative Medicine of CHU de Quebec Research Center, Université Laval, Québec, QC G1V 0A6, Canada*

Jean-François Morin – *Département de chimie And Centre de Recherche sur les Matériaux Avancés (CERMA), Université Laval, Québec, QC G1V 0A6, Canada*

T. Jane Stockmann – *Department of Chemistry, Memorial University of Newfoundland, St. John's, Newfoundland and Labrador A1B 3X7, Canada*

Francesca M. Kerton – *Department of Chemistry, Memorial University of Newfoundland St. John's, Newfoundland and Labrador A1B 3X7, Canada; https://orcid.org/0000-0002-8165-473X Email: fkerton@mun.ca*

Stephanie L. MacQuarrie – *Department of Chemistry, Memorial University of Newfoundland and Labrador A1B 3X7, Canada; Department of Chemistry, Cape Breton University, Sydney, Nova Scotia B1P 6L2*. https://orcid.org/0000-0002-0183-6622

Table of Contents

1. Experimental

1.1. Materials

Pristine hardwood biochar was provided by MacQuarrie research group from Cape Breton University, Nova Scotia, Canada. The following chemicals potassium permanganate ($KMnO_4$), sulphuric acid (H_2SO_4), boric acid (H_3BO_3), 30% hydrogen peroxide (H_2O_2), potassium bromide (KBr), and triphenyl phosphine (PPh_3) were obtained from sources such as Fisher Scientific, Sigma-Aldrich. 3-chloropropyltrimethoxysilane (CPTMS) was obtained from TGI chemicals and trioctylphosphine was obtained from Sigma-Alrich. All solvents were purified using a solvent purification system.

1.2. Methods

1.2.1. **FT-IR spectroscopy**

FT-IR spectra are obtained using a Bruker Alpha FTIR spectrometer. The samples were prepared in KBr with a ratio of 0.2:200 (Biochar: KBr by mass) and pressed into pellets. In transmission mode, the spectra were collected from 4000 to 400 cm^{-1}, with 4 cm^{-1} resolution and 24 scans for each collection. The spectra were corrected against a pure KBr pellet, and data were processed using OPUS data software.

1.2.2. **Solid-state NMR spectroscopy**

All ^{1}H, $^{13}C\{^{1}H\}$ and $^{31}P\{^{1}H\}$ CPMAS SSNMR spectra were observed at 298 K using a Bruker Avance II 600 MHz NMR spectrometer, equipped with a SB Bruker 3.2 mm magic angle spinning (MAS) triple-tuned probe operating at 600.29 MHz for ^{1}H, 150.93 MHz for $^{13}C\{^{1}H\}$, and 243.00 MHz for $^{31}P\{^{1}H\}$ nuclei. The samples were spun at 20 kHz for $^{13}C\{^{1}H\}$, and 10 kHz for $^{31}P\{^{1}H\}$. Cross-polarization (CPMAS) spectra were collected with a Hartmann-Hahn match at 62.5 kHz and 100 kHz ^{1}H-decoupling, a contact time of 2 ms and a recycling time of 5s. 8k scans (7 h) were collected for ^{13}C and 1k scans (1.5 h) for ^{31}P. Spectra were referenced externally to adamantane for $^{13}C\{^{1}H\}$ and ADP for $^{31}P\{^{1}H\}$. A known mass of triphenylphosphine (PPh_3) was also added to the samples to estimate the %P on the surface of biochar.

1.2.3. **Solution-state NMR spectroscopy**

^{1}H, ^{13}C and ^{31}P NMR spectra were obtained on a Bruker Avance 300 MHz spectrometer at 298 K, with samples prepared in distilled $CDCl_3$. Chemical shifts are reported as ppm values and referenced to the residual protons and ^{13}C in $CDCl_3$, and referenced to residual ^{31}P from trioctylphosphine in $CDCl_3$.

1.2.4. **Surface contact angle measurement**

The surface contact angle measurements were completed using a homemade setup following the same method reproduced by Zhang et al. with a hydrophobic biochar.[1] Samples were ground up to make a uniform particle size and pressed into a pellet using

a pellet press with a 39.2–39.8 % RH. The relative humidity ranged from 39.2–39.8 %, and a 10 µL drop of deionized water was added to the smoothed surface; a picture was taken where the camera was level to the flat surface, and the contact angle was measured using J.js image processing software.[2]

1.2.5. **X-ray photoelectron spectroscopy**

Chemical composition of P1 and HGNR was investigated by X-Ray Photoelectron Spectroscopy (XPS). The sample was analyzed with a PHI 5600-ci spectrometer (Physical Electronics, Eden Prairie, MN, USA). An achromatic aluminum X-ray source (1486.6 eV) was used to record the survey spectrum (1200-0 eV). High-resolution (HRXPS) spectrum on C1s peak) was obtained using an achromatic magnesium X-ray source (1253.6 eV). No charge neutralization was applied for both survey and highresolution spectra

1.2.6. **Scanning electron microscopy-energy dispersive x-ray**

Scanning electron microscopy (SEM) image of $(C_8H_{17})_3P^+Cl^-$ biochar were obtained using an FEI Quanta 400 FEG under a high vacuum (10–6 torr). The voltage was 25 kV with an electron dispersive X-ray detector (EDX).

1.2.7. **Thermal gravimetric analysis**

TGA was performed using a TA Instruments Q500 TGA under high resolution 181 dynamic mode. Approximately 20 mg of sample were heated at a rate of 10 °C/min under N2 gas flow of 50 mL/min from room temperature to 800 °C.

2. Preparation of modified biochars

Each of the following reactions was completed in a Radley carousel 12 Plus reaction station unless otherwise specified.

2.1. **Synthesis of oxidized biochar**

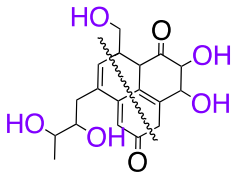

Procedure: Oxidized biochar was prepared by a modified Hummers' method.[3,4] In a three-neck round bottom flask, pristine hardwood biochar (1.01 g) is suspended in H_2SO_4 (10.0 mL) and is sonicated for 30 min. Next, the mixture is cooled in an ice bath until the temperature of the flask is below 10 ℃, and $KMnO_4$ (1.00 g, 6.33 mmol) is added slowly. Upon complete transfer, boric acid (1.6 mg, 0.03 mmol) is added, and suspension is stirred for 2 h. Deionized H_2O (25.0 mL) is added dropwise, the ice bath is switched with a silicon oil bath, and the reaction mixture is refluxed for 30 min. The suspension is cooled to room temperature, and H_2O_2 (1.2 mL) is added dropwise to the mixture. The resulting mixture is suction filtered, and the black solid is washed with HCl (1M, 6 mL), H_2O (5 mL)

and EtOH (6 mL). The oxidized biochar (0.86 g, 85% mass recovered) is dried overnight in a vacuum oven at 50 ℃ to recover a black powdery solid. ν_{max}/cm^{-1}: 3419br and 1699w (OH), 1597vs and 869w (C=C), 1200vs and 1040m (CO).

2.2. **Exfoliated oxidized biochar.**

Procedure: In a 1000 mL round bottom flask, oxidized biochar (2.00 g) is suspended in ethyl acetate (500 mL); the mixture is sonicated for 30 min, and the solid settles for 30 min.[6] The suspended exfoliated oxidized biochar was siphoned off and dried under reduced pressure. Additional ethyl acetate was added to the remaining oxidized biochar that had settled in the round bottom flask, and the procedure was repeated until all oxidized biochar was exfoliated.

2.3. **Synthesis of CPTMS biochar**

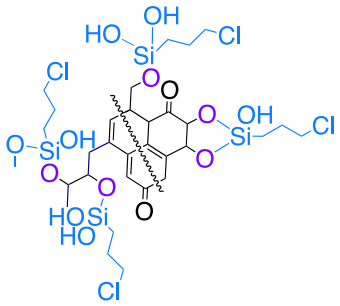

Procedure: Exfoliated and non-exfoliated hydroxylated hardwood biochar (200 mg) is suspended in anhydrous toluene (6.00 mL). Next, 3-chloropropyltrimethoxysilane, CPTMS, (0.62 g, 3.13 mmol) is added dropwise; the solution is refluxed and stirred for 24 h under a N_2 atmosphere. Finally, the reaction mixture was suction filtered, washed with toluene (3 × 20.0 mL), EtOH (1 × 10.0 mL) and solvent removed *in vacuo.* The resulting CPTMS-biochar (169 mg, 85% mass recovered) was a black powdery solid. ν_{max}/cm^{-1}: 3401br and 1700w (OH), 2894w (CH), 1597vs and 829w (C=C), 1237vs and 1018m (C–O), 1165vs (C–Si), 729w (Si–O), 692 (C–Cl). δC (600 MHz, solid) 127.8 (6 C, m, *aromatic*), 53.5 (2 C, s, *CH_2–Si* or *–O*), 21.2 (1 C, s, *CH_2*).

2.4. **Synthesis of 3-(trioctylphosphonium chloride)propyltrimethoxysilane (TOPPTMS Cl^-)**

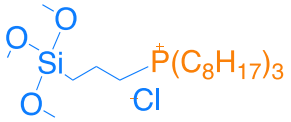

Procedure: The following procedure is modified by using acetonitrile as the solvent instead of toluene.[5] CPTMS (1.00 mL, 5.50 mmol) is suspended in anhydrous acetonitrile (8.00 mL), trioctylphosphine, TOP, (7.30 mL, 16.5 mmol) is added dropwise, and the reaction mixture is refluxed and stirred under N_2 for 96 h. The organic layer is air dried under vacuum to yield TOPPTMS Cl^- (2.62 g, 84%) as a clear colourless oil. ν_{max}/cm^{-1}: 2924vs (CH_3), 2852vs (C–H), 1088vs (Si–C), 1035vs (CO) and 919w The P–CH_2 band at 919 cm^{-1}.**δ**H (300 MHz, $CDCl_3$) 3.56 (9 H, m, *SiOMe*), 2.38 (2 H, m, *PCl–CH_2*), 1.90 (2 H, m, *Si–CH_2*), 1.71-1.62 (6 H, m, *P–CH_2*), 1.58–1.48 (12 H, m, *CH_2*), 1.26 (24 H, m, *CH_2*), 0.86 (9 H, t, *J= 6.0 Hz*, *CH_3*), 0.70 (2 H, m, *CH_2*). **δ**P (300 MHz, $CDCl_3$):**δ** 32.15 (1 P, s, *$R_3´R´´P^+$*).

2.5. **Synthesis of $(C_8H_{17})_3P^+Cl^-$ biochar**

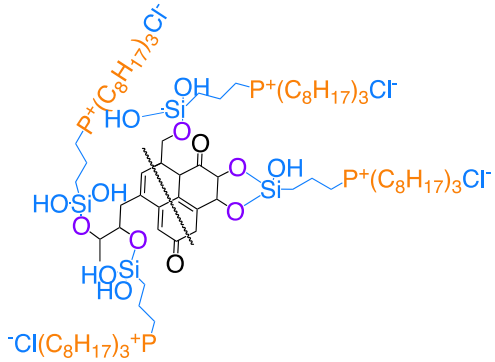

Procedure 1: CPTMS-biochar (308 mg) is suspended in anhydrous. toluene (8.00 mL). Next, TOP (1.40 mL, 3.14 mmol) is added slowly dropwise to the reaction mixture. This reaction mixture was refluxed and stirred under N_2 for 96 h. Upon reaction completion, the mixture is suction filtered; the solid is washed with toluene (2 × 10.0 mL) and EtOH (2 × 10.0 mL). The black powdery solid is dried *in vacuo* and identified as the indirect synthesis of $(C_8H_{17})_3P^+Cl^-$ biochar (253 mg, 82%).

Procedure 2: TOPPTMS Cl^- (885 mg, 1.55 mmol) is suspended in anhydrous toluene (4.00 mL). Next, exfoliated hydroxylated biochar (205 mg) is added; this mixture is refluxed and stirred under N_2 for 24 h. Upon reaction completion, the mixture is the suction filtered; the solid is washed with toluene (2 × 20.0 mL) and EtOH (2 × 20.0 mL). The black powdery solid is dried under reduced pressure and identified as the direct synthesis of $(C_8H_{17})_3P^+Cl^-$ biochar (152 mg, 74%).

Characterization data: ν_{max}/cm^{-1}: 3435vb and 1700wb (OH); 2919w (CH_3), 2846 (C–H), 1577vs and 877w (C=C); 1226vs and 1052w (CO); 1165vs (C–Si), 729w (Si–O), 692w (C–Cl). δC (600 MHz, solid) 127.2 (6 C, m, *aromatic*), 73.8 (1C, m, *CH_2-PCl*), 50.8 (1 C, s, *CH_2–Si* or *–O*), 31.0 (3 C, m, *CH_2-P*), 29.1 (6 C, m, *CH_2*), 27.2 (6 C, m, *CH_2*), 23.2 (1 C, s, *CH_2*), 14.8 (9 C, m, *CH_3*). δH (600 MHz, solid) 5.2 (2 H, bs, C=CH_2), 4.2 (H, bs), 4.0 (H, bs), 2.7 (2 H, m, *PCl–CH_2*), 2.1 (6 H, m, CH_2), 1.9 (2 H, m, *Si–CH_2*), 1.5 (12 H, m, *CH_2*), 1.2 (24 H, m, *CH_2*), 0.77 (9 H, bs, *CH_3*). **δ**P (600 MHz, solid): 31.5 (1 P, s, *$R_3'R''P^+$*).

3. FT-IR spectroscopy studies

3.1. **Oxidized biochar**

EtOAc was chosen to exfoliate hydroxylated biochar due to its hydrogen bond acceptor stabilizing effects.[6] The –OH groups on the surface of the hydroxylated biochar are stabilized by EtOAc, producing stacked monolayers instead of highly aggregated hydroxylated biochar. This should increase the number of accessible sites for modification, improve biochar dispersity in solution and decrease overall surface area.

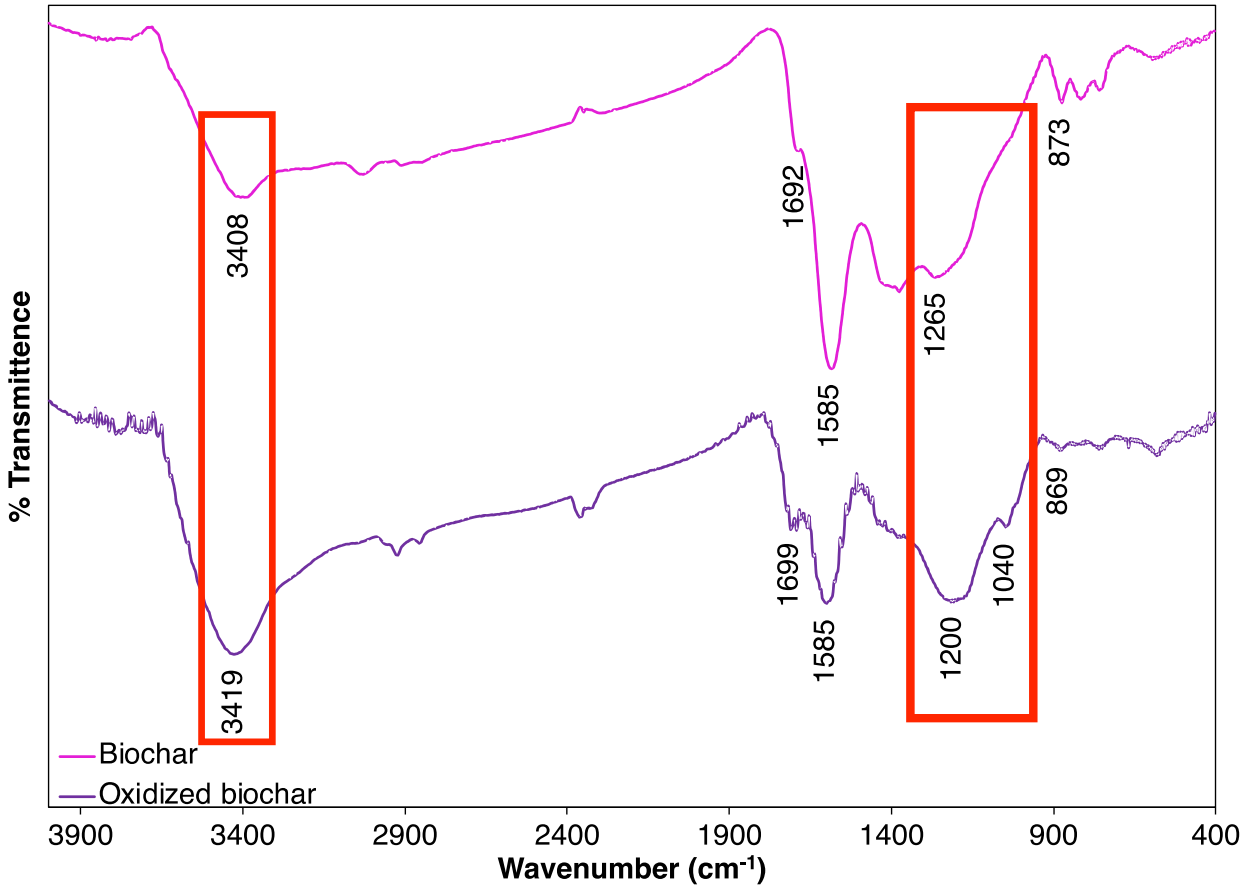

Figure S 1 FT-IR spectra of pristine hardwood biochar (pink, top) and oxidized biochar (purple, bottom).

3.2. **CPTMS biochar**

Without knowing the degree of hydroxylation of the surface of biochar, the optimizations of the CPTMS condensation were attempted by differing the amounts of CPTMS reagent added to the reactions to 3 eq, 7 eq and 9 eq (w/w) on both exfoliated and non-exfoliated oxidized biochar. The optimized CPTMS biochar via CPTMS condensation was achieved using 9 equivalents (w/w) on both exfoliated and non-exfoliated oxidized biochar. (Fig. 1(iv)).

Table S 1 Reaction optimization study of the synthesis of CPTMS biochar from oxidized biochar.

Eq of CPTMS	Exfoliation	Oxidized biochar(mg)	CPTMS biochar (mg)

3	yes✔	202	147
3	no	205	170
7	yes✔	203	159
7	no	202	176
9	yes✔	201	163
9	no	204	169

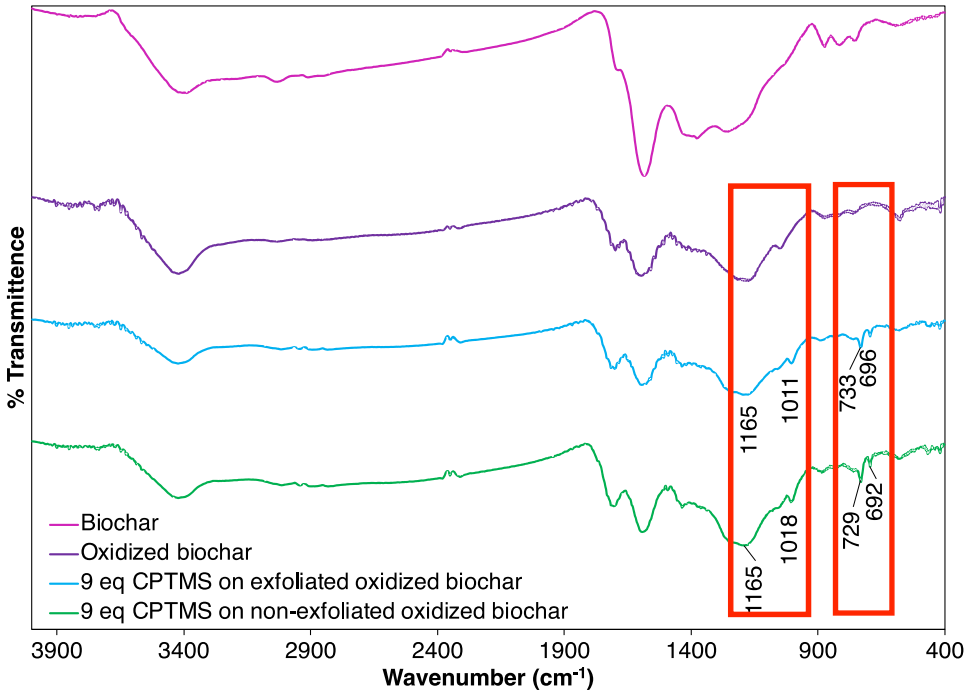

Figure S2 FT-IR spectra of biochar (pink, top), hydroxylated biochar (purple, middle 1), and 9 eq exfoliated CPTMS-biochar (blue, middle 2) and 9 eq of non-exfoliated CPTMS-biochar (green, bottom).

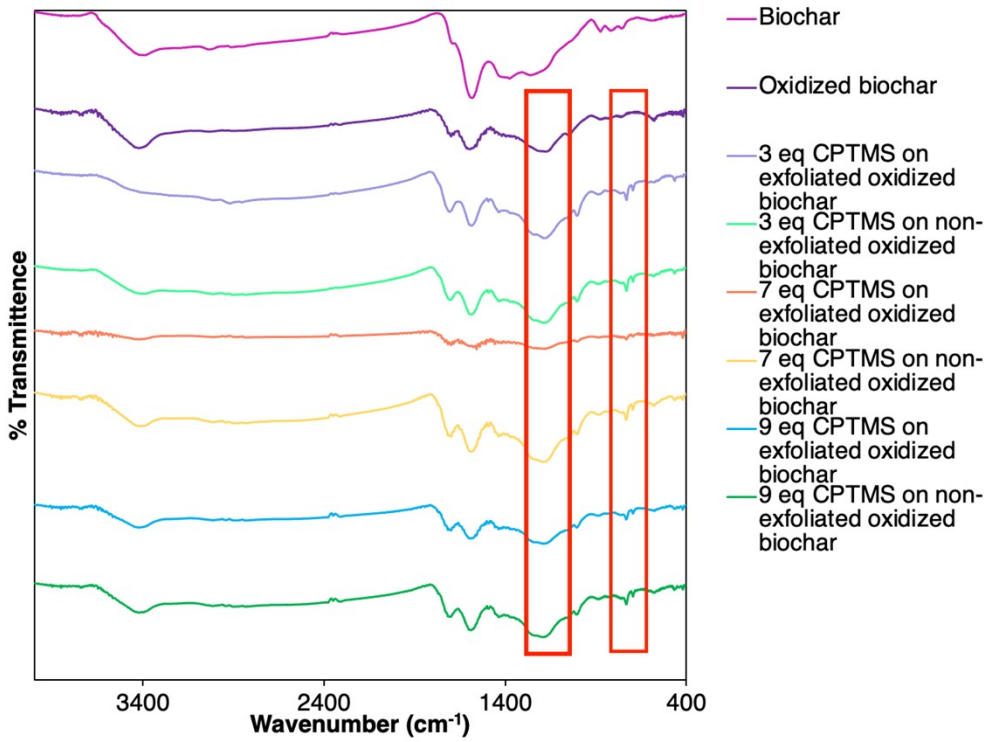

Figure S3 FT-IR spectra of CPTMS biochar optimization.

3.3. **TOPPTMS Cl^-**

There was no significant difference in exfoliated and non-exfoliated biochar with each equivalence of CPTMS. Therefore, 9 eq of CPTMS was selected so that an excess could be used in the reaction. (**Figure 3**) The most significant change in the FT-IR spectrum is the added peaks at 696 cm^{-1} and 733 cm^{-1}, representing the C–Cl and Si–C stretches, respectively. (**Figure 2**)

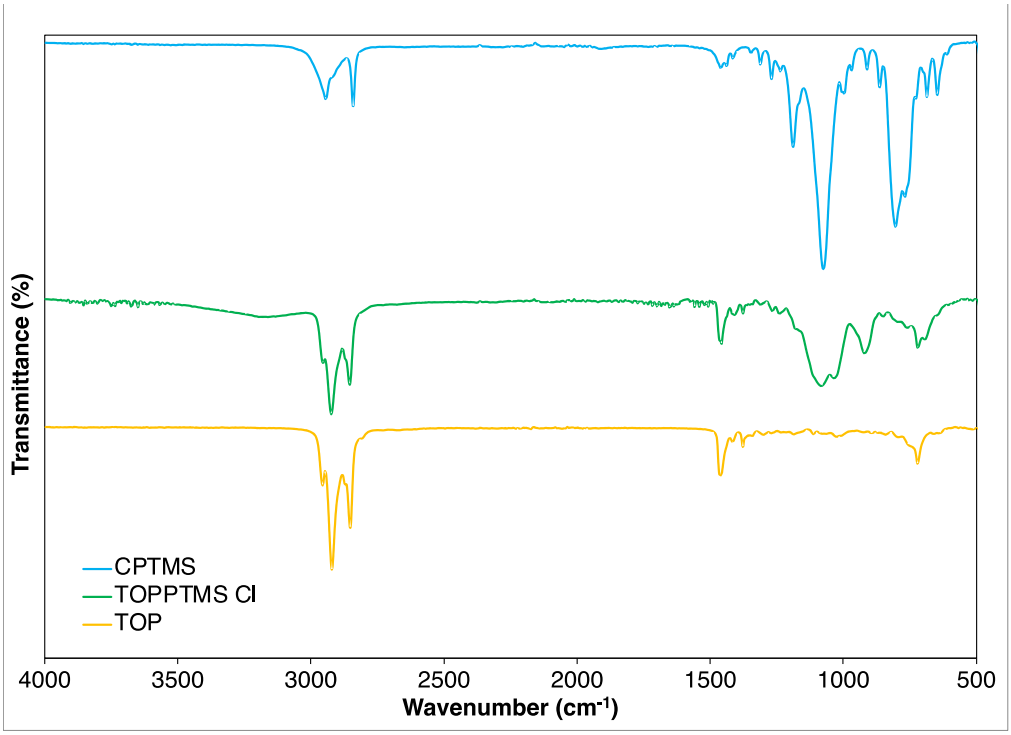

Figure S4 Stacked FT-IR spectra of CPTMS (blue, row 1), TOPPTMS Cl^- (green, row 2) and TOP (yellow, row 3).

3.4. $(C_8H_{17})_3P^+Cl^-$ biochar

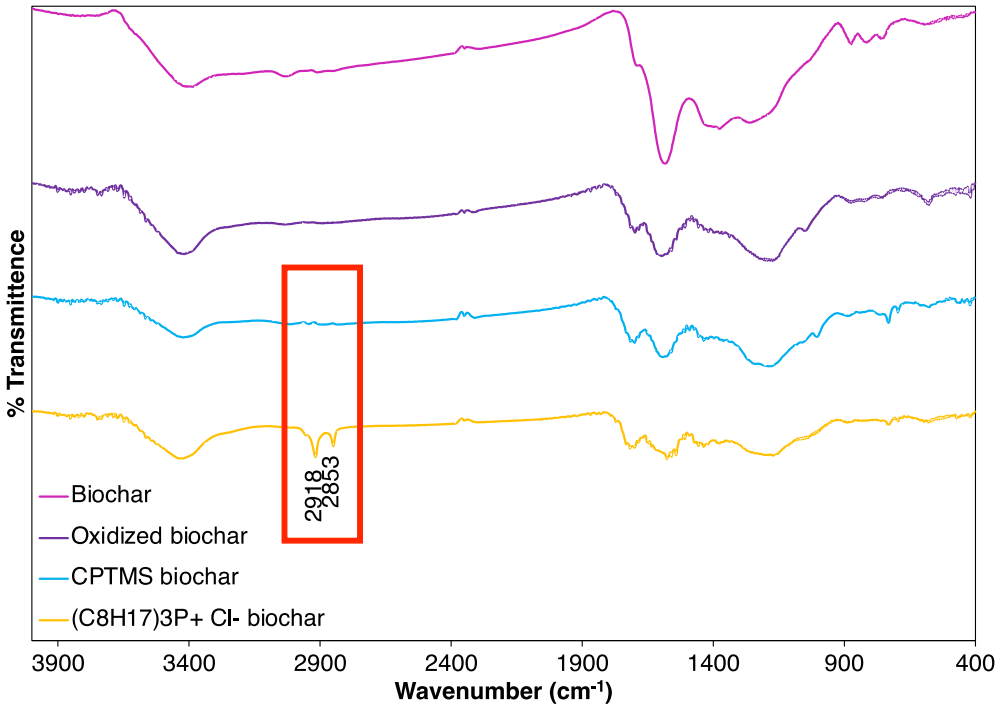

Figure S5 Stacked FT-IR spectra of pristine biochar (pink, row 1), hydroxylated biochar (purple, row 2), CPTMS-biochar (blue, row 3,), and $(C_8H_{17})_3P^+Cl^-$ biochar (orange, row 4).

3.5. **Alternative direct synthetic route to phosphonium-modified biochar**

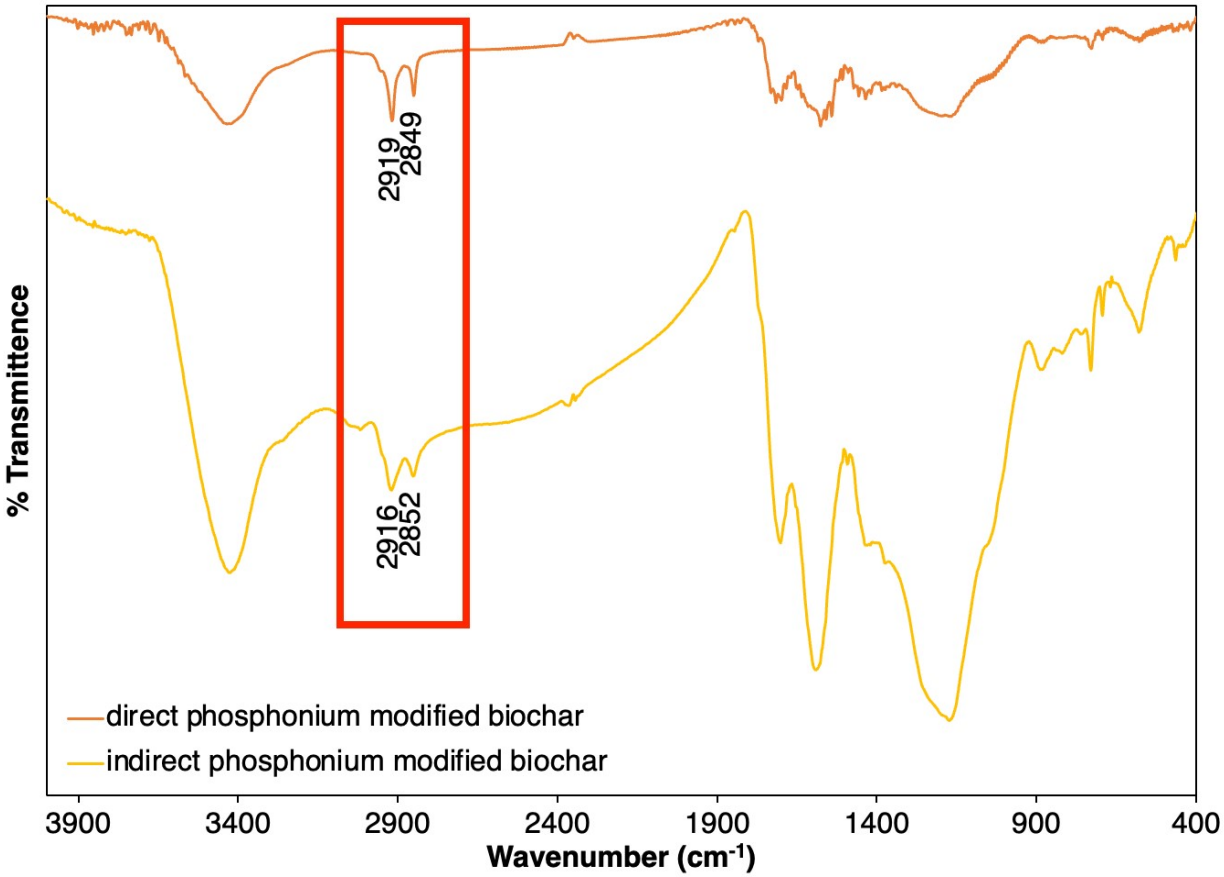

Figure S6 The FT-IR spectra of exfoliated $(C_8H_{17})_3P^+Cl^-$ biochar using direct synthesis (orange, top) and indirect synthesis (yellow, bottom) routes.

Table S2 Reaction optimization for the synthesis of $(C_8H_{17})_3P^+Cl^-$ biochar from CPTMS biochar for 96 h.

Eq of $(P(Oc)_3)$	Exfoliation	CPTMS biochar (mg)	$(C_8H_{17})_3P^+Cl^-$ biochar (mg)
3	Yes✔	49.2	26.0
3	No	49.2	21.2
6	Yes✔	48.9	28.5
6	No	49.1	19.3
9	Yes✔	50.3	31.1
9	No	52.4	19.1

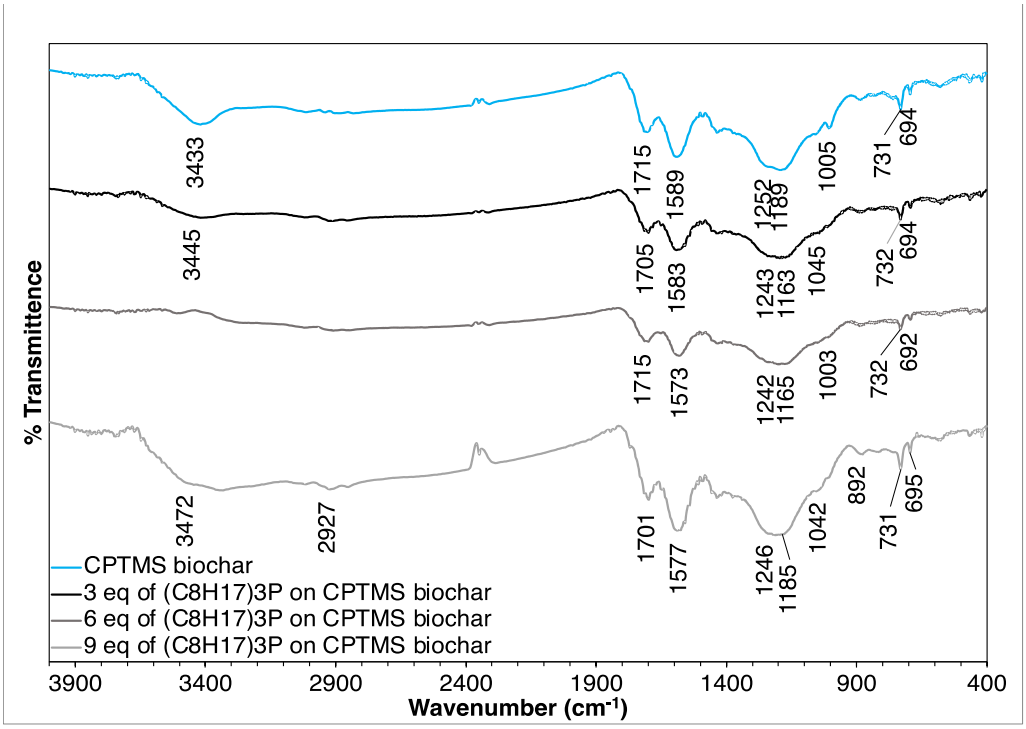

Figure S7 Stacked FT-IR spectra of 48 h phosphonium modification reaction on non-exfoliated biochar.

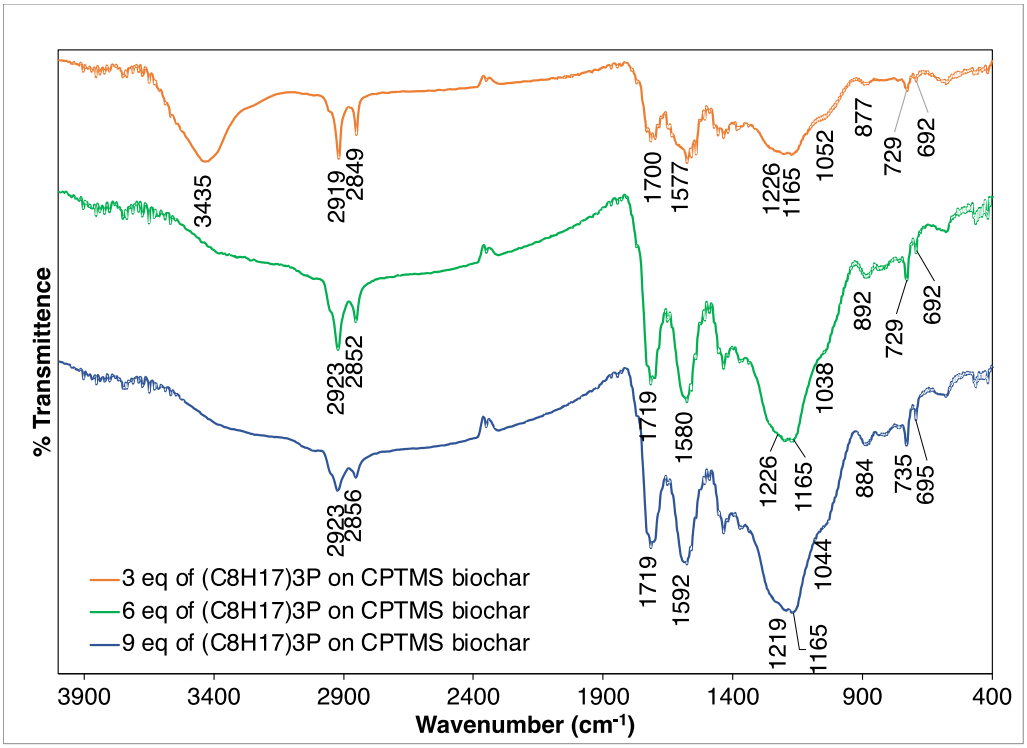

Figure S8 Stacked FT-IR spectra of 3, 6 and 9 eq of TOP (w/w) applied to CPTMS biochar to synthesize $(C_8H_{17})_3P^+Cl^-$ biochar over 96 h.

4. NMR studies

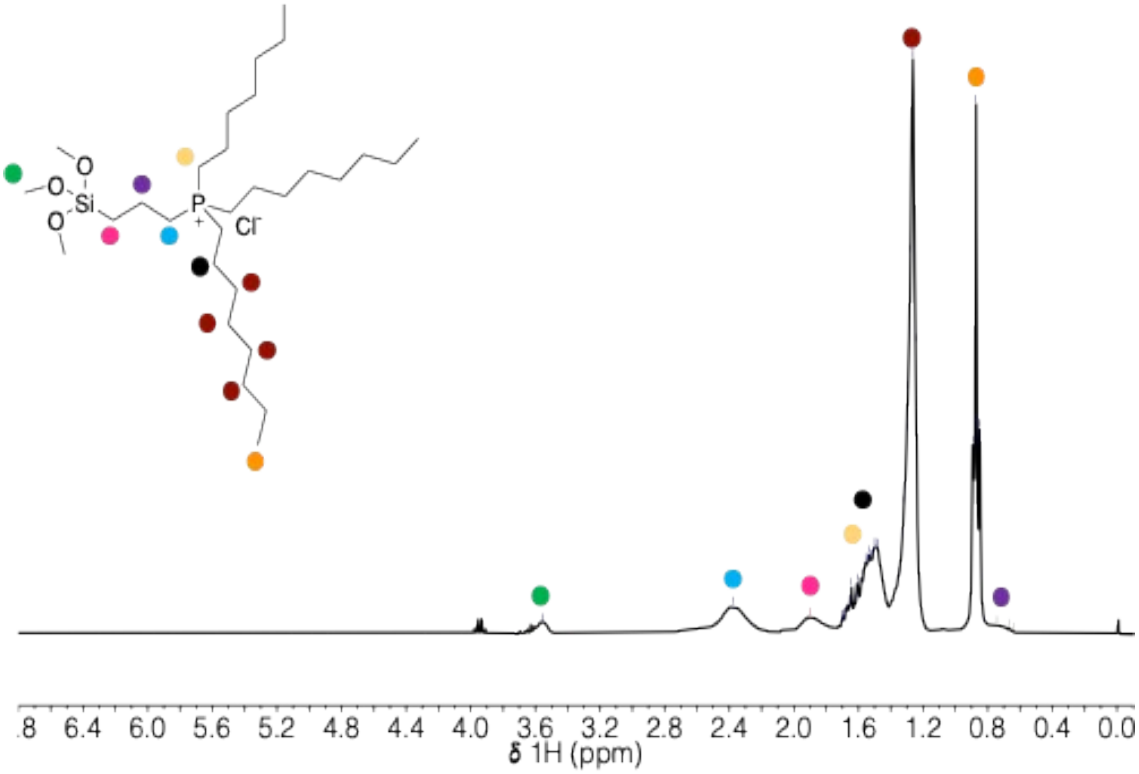

Figure S9 TOPPTMS Cl^- in solution ^1H NMR (300 MHz, $CDCl_3$) δ **δ**H (300 MHz, $CDCl_3$) 3.56 (9 H, m, *SiOMe*), 2.38 (2 H, m, *PCl–CH$_2$*), 1.90 (2 H, m, *Si–CH$_2$*), 1.71-1.62 (6 H, m, *P–CH$_2$*), 1.58–1.48 (12 H, m, *CH$_2$*), 1.26 (24 H, m, *CH$_2$*), 0.86 (9 H, t, *J= 6.0 Hz*, *CH$_3$*), 0.70 (2 H, m, *CH$_2$*) ppm. Dots on the spectrum represent H atoms in TOPPTMS Cl^-

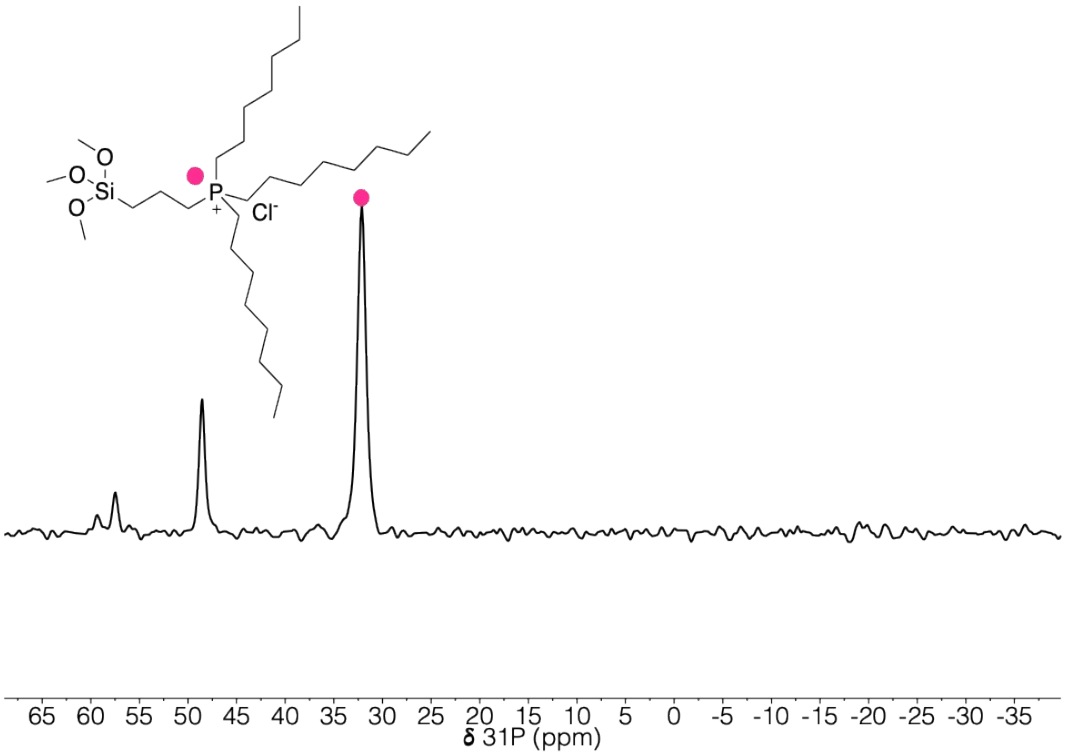

Figure S10 TOPPTMS Cl^- in solution ^{31}P NMR (122 MHz, $CDCl_3$) δ 49, 32 ppm. Dots on the spectrum represent P atom in TOPPTMS Cl^-

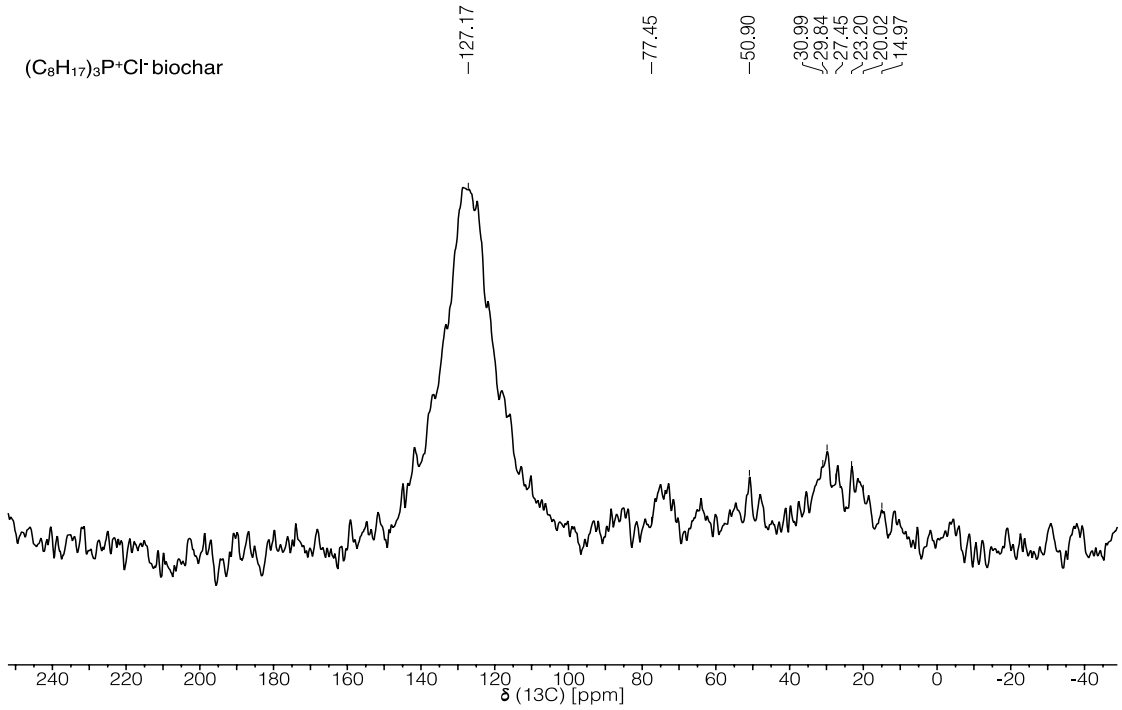

Figure S11 $^{13}C\{1H\}$ CPMAS NMR spectrum of $(C_8H_{17})_3P^+Cl^-$ biochar collected at 600 MHz, vr=20 kHz, ns=8 k.

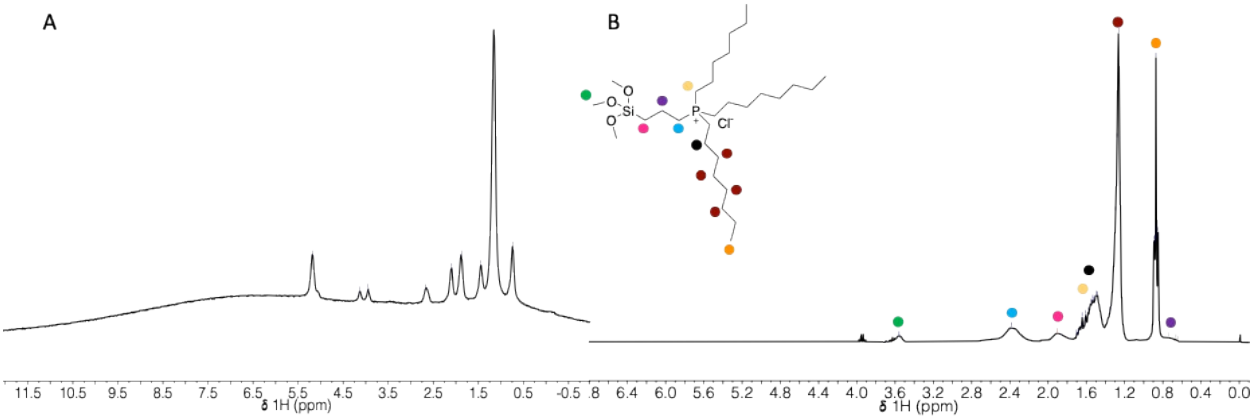

Figure S12 Left: ^{1}H MAS NMR of $(C_8H_{17})_3P^+Cl^-$ biochar (A) collected at 600 MHz, vr=20 kHz, ns=8K. Right: TOPPTMS Cl^- (B) in solution ^{1}H NMR (300 MHz, $CDCl_3$) 3.56 (9 H, m, *SiOMe*), 2.38 (2 H, m, *PCl–CH*$_2$), 1.90 (2 H, m, *Si–CH*$_2$), 1.71-1.62 (6 H, m, *P–CH*$_2$), 1.58–1.48 (12 H, m, *CH*$_2$), 1.26 (24 H, m, *CH*$_2$), 0.86 (9 H, t, *J= 6.0 Hz*, *CH*$_3$), 0.70 (2 H, m, *CH*$_2$) ppm. Dots on the spectrum represent H atoms in TOPPTMS Cl^-

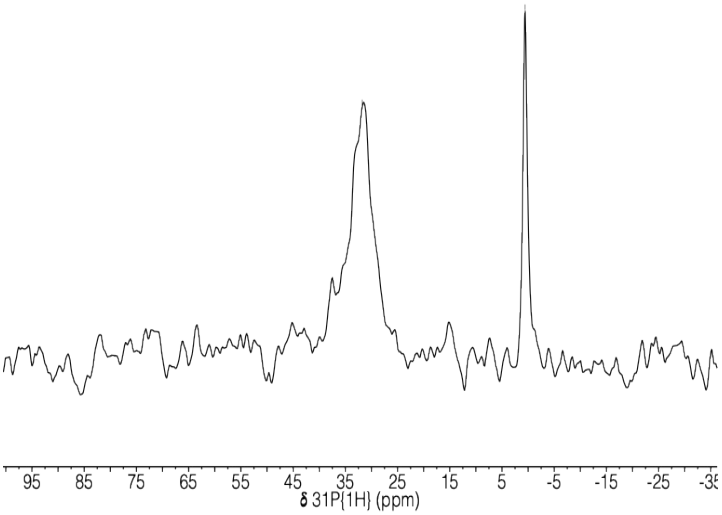

Figure S13 $^{31}P\{1H\}$ CPMAS NMR spectrum of indirect graft non-exfoliated $(C_8H_{17})_3P^+Cl^-$ biochar collected at 243 MHz, vr=10 kHz, ns=1k. ADP (0.58, 1 P) used as the internal reference.

5. Surface contact angle measurement

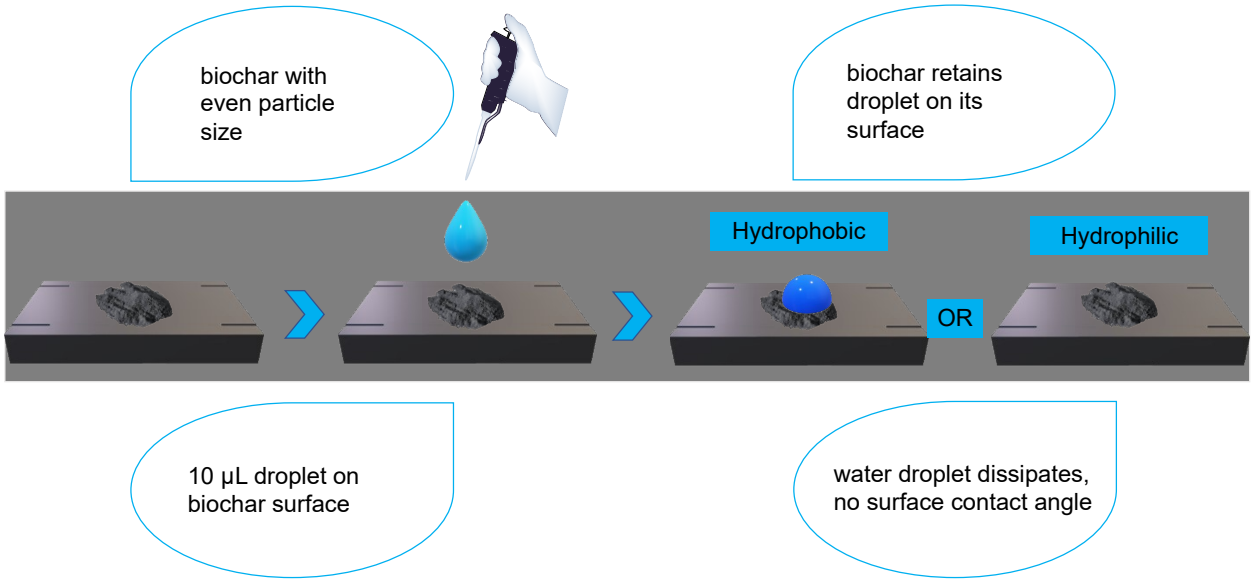

Figure S14 Experimental process for determining the hydrophobicity of $(C_8H_{17})_3P^+Cl^-$ biochar.

Figure S15 Surface contact angle experimental setup

Figure S16 The contact surface angle measurements of exfoliated indirect graft of $(C_8H_{17})_3P^+Cl^-$ biochar.

Above photos represent each of the pictures taken for each of the different samples of $(C_8H_{17})_3P^+Cl^-$ biochar that was used to determine angle of hydrophobicity, text was added during sample analysis to stay organized.

6. Quantification of Phosphorus on biochar

Calculations of the quantification of phosphorus on the surface of biochar. Non-exfoliated biochar is used for sample calculations.

Calculation of n_{PPh3}

n_{PPh3}=0.01919 g / 262.29 g/mol = 7.31 mmol = 7.31 mmol of phosphorus.

$$n_{PPh3} = \frac{mass\ of\ PPh3}{Mm\ of\ PPh3} = \frac{0.01919 g}{262.\ g/mol} = 7.31\ mmol\ per\ mol\ of\ PPh3$$

$$n_{P,BC} = n_{PPh3} \bullet \frac{0.16}{1.00} = 7.31\ mmol \bullet 0.16 = \ 11\ \mu mol\ of\ P\ in\ 26.77\ mg\ sample.$$

$$m_{PBC} = n_P \bullet Mm_{P,\ atomic\ mass} = 1.10X10^5 mol \bullet 30.97\ g/mol = 0.341\ mg\ of\ P$$

$$m\%_{P,BC} = \frac{mass\ of\ P\ in\ samples}{total\ mass\ of\ P\ biochar} \bullet 100\% = \frac{0.341\ mg}{26.77\ mg} \bullet 100\% = 1.3\ \%\ P$$ functionalization.

Sample 2: 7.5e-05 mol (2.32 mg P) in 20 mg sample= 11.6 % P functionalization

Sample 3: 1.19E-04 mol (3.69 mg P) in 20.5 mg sample 18.0% P functionalization

7. XPS analysis of exfoliated direct and indirect $(C_8H_{17})_3P^+Cl^-$ biochars

We further characterized the exfoliated direct and indirect $(C_8H_{17})_3P^+Cl^-$ biochar by XPS to confirm functionalization. Figure S17 and S18 A-D represents the high-resolution XP spectra, and E is the XP survey scan for each modified biochar. For the C1s spectra of exfoliated indirect and direct graft of $(C_8H_{17})_3P^+Cl^-$ biochar, the signals at 284, 284.4, 285, 286.3 and 288.2 eV represents the bond environments for sp^3 C, C=C, C–H & C–C, C-OH & O–C–O and (C=O)O–Si, respectively (figure S17 and S18).[7,8] The (C=O)O–Si signal (288.2 eV) confirms the anchoring of silane on biochar surface.[8,9] The Si 2p signals that correspond to Si–C and SiO_2 are 102.2 eV and 103.3 eV, respectively, representing the CPTMS linker between the biochar surface and the phosphonium ionic liquid.[8,9] The P 2p spectra of both species, the peaks at 132.5 and 134.2 eV are observed ascribes to the P $2p_{3/2}$ and $2p_{1/2}$ of the quaternary phosphonium salt.[10] While these results further evidence the successful modification of biochar, these results are complex and quaternary salts are not well characterized by XPS in the literature. This demonstrates an additional limitation that can be overcome by using solid-state NMR spectroscopy.

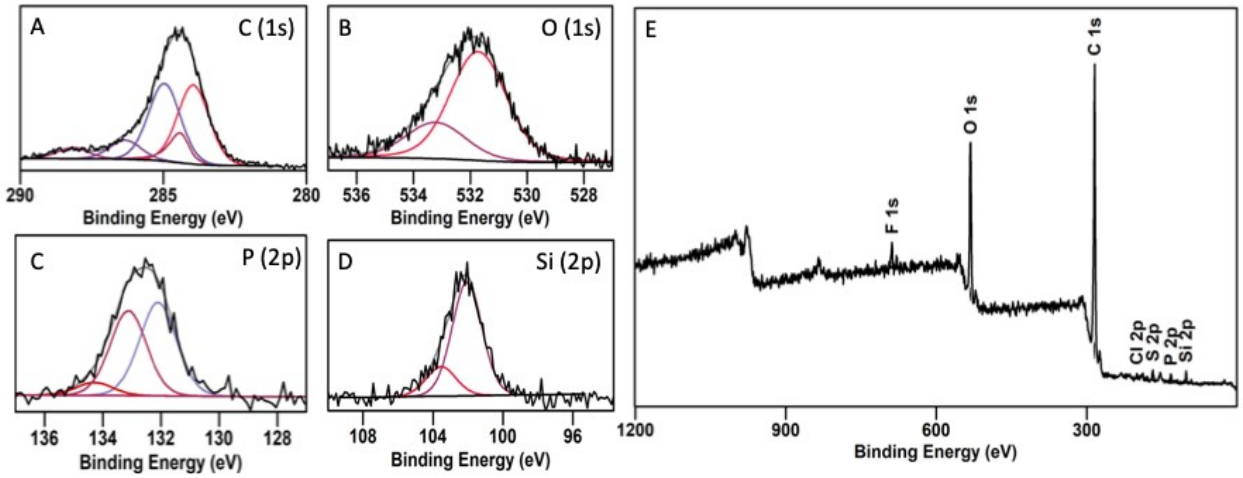

Figure S17 XP spectra of C 1s (A),O 1s (B), P 2p (C), Si 2p(D) and XP survey spectra (E) of exfoliated direct graft $(C_8H_{17})_3P^+Cl^-$ biochar.

Table S3 Atomic composition (%) of different XP signals from the XP survey spectrum of exfoliated direct graft $(C_8H_{17})_3P^+Cl^-$ biochar.

Signal	BE (eV)	FWHM	%At Conc
O 1s	531.6	3.5	16
C 1s	284.4	2.8	76.6
F 1s	688.4	2.6	1.3
Cl 2p	200.4	2.8	0.4
Si 2p	102.00	2.2	3.0
P 2p	132.4	2.6	1.4
S 2p	168.4	3.0	1.4

Table S4 Relative composition of different XP signals from the high-resolution XP spectra of exfoliated direct graft $(C_8H_{17})_3P^+Cl^-$ biochar.

Signal	BE (eV)	FWHM	%At Conc
Sp^3 C	284	1.3	19.86
(C=O)O–Si	288.2	1.3	2.71
C=C	284.4	0.7	5.71
C–OH, O–C–O	286.3	1.3	4.78
C–H, C–C	285	1.3	19.54
Si–O	531.7	2.3	28.92
C–OH (aromatic)	533.2	2.5	10.29
2P 3/2	132.1	1.5	0.59
2P 1/2	134.3	1.5	0.08
2P 3/2 (alkyl)	133.1	1.5	0.52
Si–O	103.5	2	0.31
Si–C	102.1	2	1.18

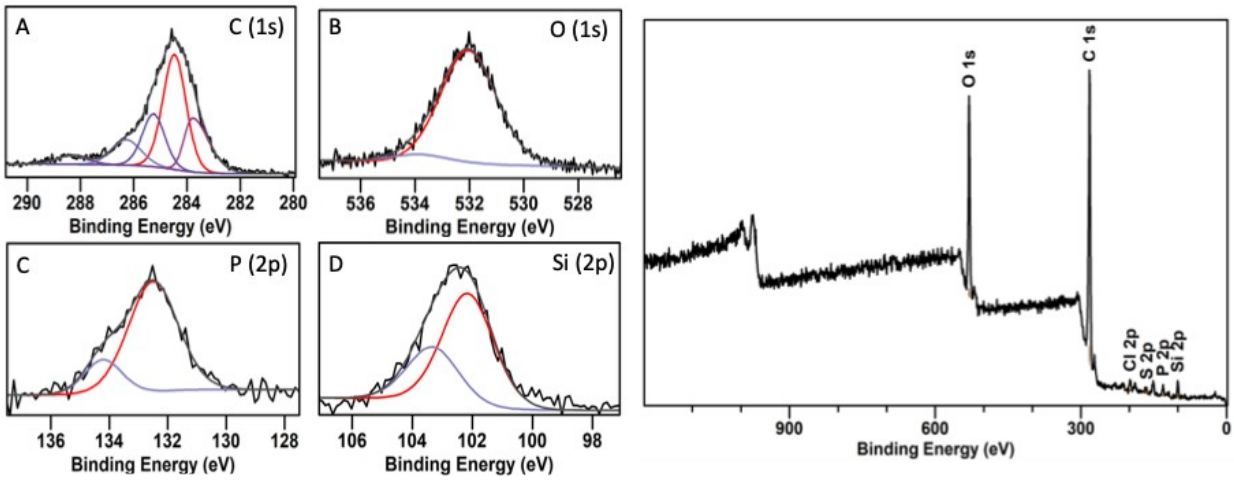

Figure S18 XP spectra of C 1s (A),O 1s (B), P 2p (C), Si 2p (D) and XP survey spectra (E) of exfoliated indirect graft $(C_8H_{17})_3P^+Cl^-$ biochar.

Table S5 Atomic composition (%) of different XP signals from the XP survey spectrum of exfoliated indirect graft $(C_8H_{17})_3P^+Cl^-$ biochar.

Signal	BE (eV)	FWHM	%At Conc
O 1s	532	3.4	16.4
C 1s	284.6	3.4	77
Cl 2p	200.7	3.2	0.6
Si 2p	103.1	3.1	4.3
P 2p	132.7	2	1
S 2p	166.3	3.9	0.7

Table S6 Relative composition of different XP signals from the high-resolution XP spectra of exfoliated indirect graft $(C_8H_{17})_3P^+Cl^-$ biochar.

Signal	BE (ev)	FWHM	%At Conc
C=C	284.5	1	25.2
C–O–C, C–OH	286.3	1.3	7.1
Sp^3 C	283.8	0.8	13
(C=O)O–Si	288.3	1.3	2.6
C–C, C–H	285.3	1	11.3
Si–O	532	2.4	35.4
C–OH (aromatic)	533.8	2.4	0.9
2P 3/2	132.5	2	1
2P 1/2	134.2	1.5	0.3
Si–C	102.2	2	1.8
Si–O	103.3	2	0.9

8. SEM-EDX analysis

The exfoliated indirectly grafted $(C_8H_{17})_3P$+Cl- biochar was analyzed by SEM-EDX to try to quantify the phosphonium functional groups added to biochar's surface. We approached this by obtaining the elemental composition of several pieces of the modified biochar. In Table S7, there is an extremely low amount of phosphorus, P, present at each point along with a higher amount of silicon, Si. It should be noted that biochar naturally contains silicon.

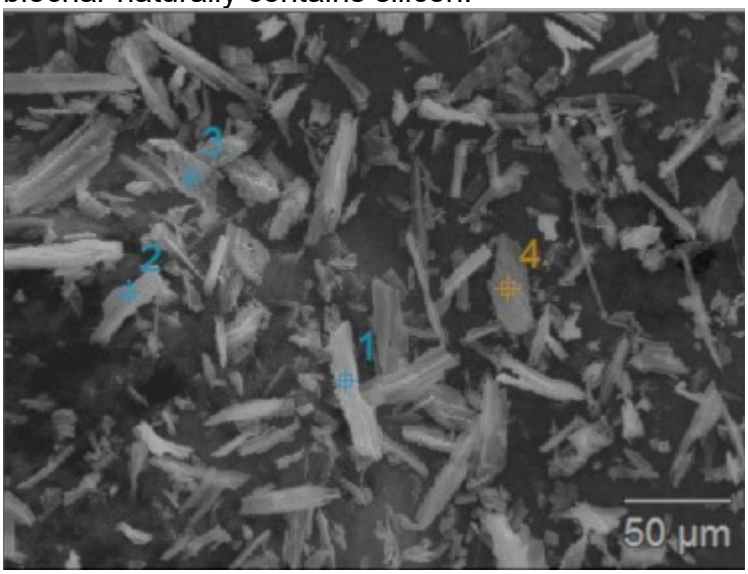

Figure S19 SEM-EDX of exfoliated indirect graft $(C_8H_{17})_3P^+Cl^-$ biochar.

Table S7 Atomic composition of different EDX points of **Figure S19** of exfoliated indirectly grafted $(C_8H_{17})_3P^+Cl^-$ biochar.

$(C_8H_{17})_3P^+Cl^-$ biochar	**C-K**	**O-K**	**Si-K**	**P-K**	**S-K**	**Cl-K**	**Ca-K**
Point 1	87.7	11.8	0.1	0.02	0.2	0.06	0.06
Point 2	88.9	10.8		0.01	0.2		0.07
Point 3	92.3	6.6	0.3	0.07	0.4	0.3	0.1
Point 4	94.9	3.8	0.2	0.07	0.8	0.1	0.1

9. TGA

Thermal gravimetric analysis was used to provide evidence of functionalization of oxidized, CPTMS and $P(C_8H_{17})_3^+Cl^-$ biochar. In Figure S19, pristine biochar demonstrates a 25% weight loss when ramped to 800 ℃. The thermogram of oxidized carbon (Figure S19, purple) presents the complete biochar combustion when ramped to temperatures of 800 ℃, demonstrating the instability created in the material via oxidation. There is a notable change when functionalized with CPTMS, this thermogram maintains a 10% weight loss in difference compared to biochar, the CPTMS biochar is stabilized again with the added CPTMS group. $P(C_8H_{17})_3^+Cl^-$ biochar is synthesized from CPTMS biochar that influences the 15% weight loss above 450 ℃ – 800 ℃ in addition to the 10% weight loss of CPTMS biochar, further confirming functionalization.

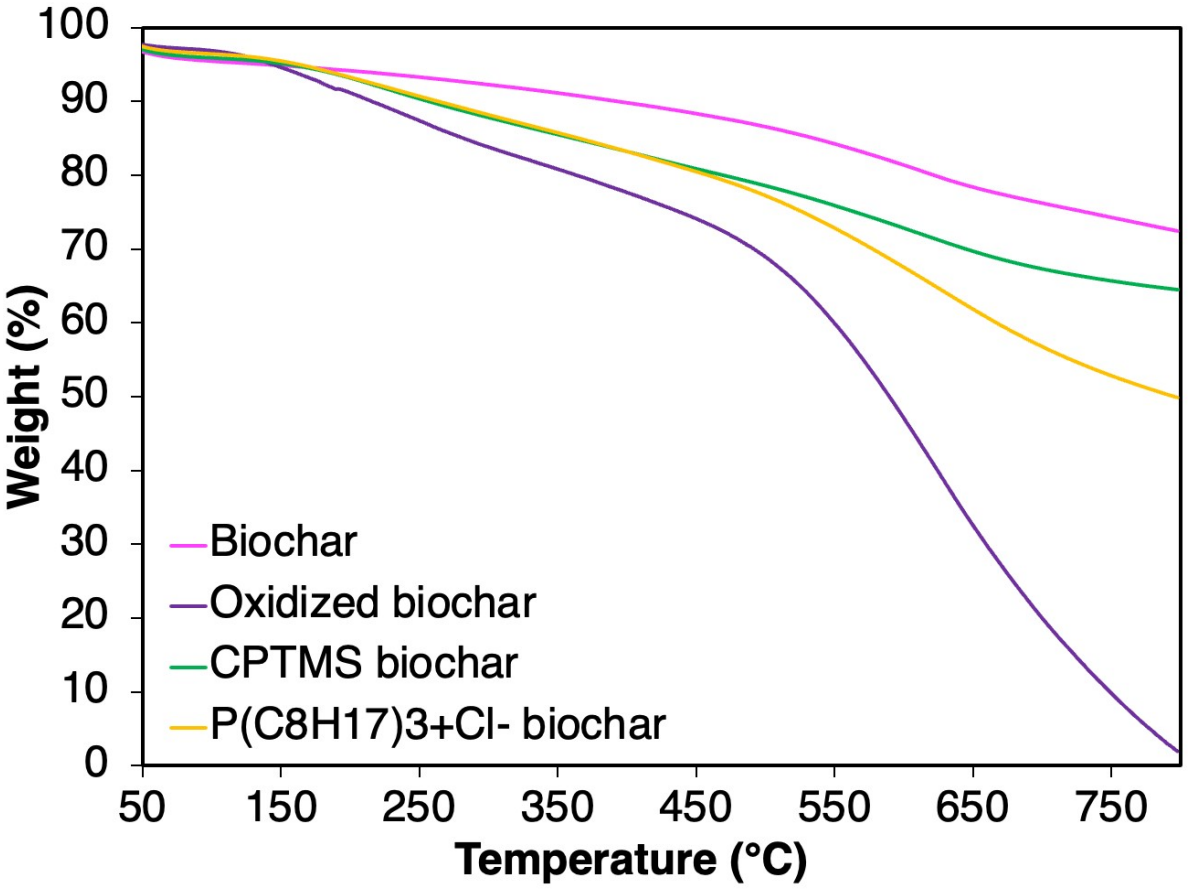

Figure S20 TGA of biochar, oxidized biochar, CPTMS biochar and $P(C_8H_{17})_3^+Cl^-$ biochar.

10. Comparison of analytical methods

Table S8 The advantages and disadvantages of surface characterization methods for proving modification on biochar.

Analysis	Advantages	Disadvantages
IR	Extremely useful for identifying functional groups[11] that demonstrate 1) metal to carbon bond vibrational modes 2) strong intensity bands	Challenge with identifying weak to medium intensity bands especially bands in the 1100–1600 cm^{-1} IR region.[12]
XPS	Probes nanoscale layers for chemical composition.[13] Useful for functional group analysis. [14]	Penetrates < 10 nm on surface. [13] Expensive. Limited by detection point of analysis since biochar is a extremely heterogeneous mixture data sets won't be consistent. [14]
SEM-EDX	Characterization and distribution of components at macro and micro scales.[15] Identifies changes to surface morphology.[14]	On the microns to centimeters scale. [15] Not useful for determining atomic % due to limited sensitivity. (< ppm)
TEM	Images on the atomic scale. [15] Extremely useful for highlighting surface morphology	Expensive.[15] Limited use of EDS in determining atomic % due to sensitivity
TGA	Determines structural stability. [14] Determines modification made to surface based on changes in thermal stability.[16]	Only sensitive on the micron scale. Only useful for characterizing modified biochar is biochar is stable up to 700℃.[14]
Solid-state NMR spectroscopy	Can be useful for identifying aliphatic, phenolic, aromatic and methoxyl and other hydrocarbons using ^{13}C ssNMR.[14]	Carbon NMR presents as a range due to various present. Broader peaks than solution-state NMR spectroscopy.

11. References

(1) Zhang, M.; Zhu, H.; Xi, B.; Tian, Y.; Sun, X.; Zhang, H.; Wu, B. Surface Hydrophobic Modification of Biochar by Silane Coupling Agent KH-570. *Processes* **2022**, *10* (2), 301. https://doi.org/10.3390/pr10020301.

(2) Image J. Js. https://ij.imjoy.io/.

(3) Hummers, W. S. Jr.; Offeman, R. E. Preparation of Graphitic Oxide. *J. Am. Chem. Soc.* **1958**, *80* (6), 1339–1339. https://doi.org/10.1021/ja01539a017.

(4) Chen, J.; Yao, B.; Li, C.; Shi, G. An Improved Hummers Method for Eco-Friendly Synthesis of Graphene Oxide. *Carbon* **2013**, *64*, 225–229. https://doi.org/10.1016/j.carbon.2013.07.055.

(5) Zhu, J. M.; Xin, F.; Sun, Y. C.; Dong, X. C. Phosphonium-Based Ionic Liquids Grafted onto Silica for CO2 Sorption. *Theor. Found. Chem. Eng.* **2014**, *48* (6), 787–792. https://doi.org/10.1134/S0040579514060141.

(6) Vidal, J. L.; Gallant, S. M. V.; Connors, E. P.; Richards, D. D.; MacQuarrie, S. L.; Kerton, F. M. Green Solvents for the Liquid-Phase Exfoliation of Biochars. *ACS Sustain. Chem. Eng.* **2021**, *9* (27), 9114–9125. https://doi.org/10.1021/acssuschemeng.1c02823.

(7) Fujimoto, A.; Yamada, Y.; Koinuma, M.; Sato, S. Origins of Sp^3 C Peaks in C_{1s} X-Ray Photoelectron Spectra of Carbon Materials. *Anal. Chem.* **2016**, *88* (12), 6110–6114. https://doi.org/10.1021/acs.analchem.6b01327.

(8) Lee, K. H.; Chu, J. Y.; Kim, A. R.; Yoo, D. J. Fabrication of High-Alkaline Stable Quaternized Poly(Arylene Ether Ketone)/Graphene Oxide Derivative Including Zwitterion for Alkaline Fuel Cells. *ACS Sustain. Chem. Eng.* **2021**, *9* (26), 8824–8834. https://doi.org/10.1021/acssuschemeng.1c01978.

(9) Gusain, R.; Mungse, H. P.; Kumar, N.; Ravindran, T. R.; Pandian, R.; Sugimura, H.; Khatri, O. P. Covalently Attached Graphene–Ionic Liquid Hybrid Nanomaterials: Synthesis, Characterization and Tribological Application. *J. Mater. Chem. A* **2016**, *4* (3), 926–937. https://doi.org/10.1039/C5TA08640J.

(10) Dai, W.; Mao, P.; Liu, Y.; Zhang, S.; Li, B.; Yang, L.; Luo, X.; Zou, J. Quaternary Phosphonium Salt-Functionalized Cr-MIL-101: A Bifunctional and Efficient Catalyst for CO2 Cycloaddition with Epoxides. *J. CO2 Util.* **2020**, *36*, 295–305. https://doi.org/10.1016/j.jcou.2019.10.021.

(11) Kasera, N.; Hall, S.; Kolar, P. Effect of Surface Modification by Nitrogen-Containing Chemicals on Morphology and Surface Characteristics of N-Doped Pine Bark Biochars. *J. Environ. Chem. Eng.* **2021**, *9* (2), 105161. https://doi.org/10.1016/j.jece.2021.105161.

(12) Tan, X.-F.; Zhu, S.-S.; Wang, R.-P.; Chen, Y.-D.; Show, P.-L.; Zhang, F.-F.; Ho, S.-H. Role of Biochar Surface Characteristics in the Adsorption of Aromatic Compounds: Pore Structure and Functional Groups. *Chin. Chem. Lett.* **2021**, *32* (10), 2939–2946. https://doi.org/10.1016/j.cclet.2021.04.059.

(13) Krishna, D. N. G.; Philip, J. Review on Surface-Characterization Applications of X-Ray Photoelectron Spectroscopy (XPS): Recent Developments and Challenges. *Appl. Surf. Sci. Adv.* **2022**, *12*, 100332. https://doi.org/10.1016/j.apsadv.2022.100332.

(14) Igalavithana, A. D.; Mandal, S.; Niazi, N. K.; Vithanage, M.; Parikh, S. J.; Mukome, F. N. D.; Rizwan, M.; Oleszczuk, P.; Al-Wabel, M.; Bolan, N.; Tsang, D. C. W.; Kim,

K.-H.; Ok, Y. S. Advances and Future Directions of Biochar Characterization Methods and Applications. *Crit. Rev. Environ. Sci. Technol.* **2017**, *47* (23), 2275–2330. https://doi.org/10.1080/10643389.2017.1421844.
(15) Brodusch, N.; Brahimi, S. V.; Barbosa De Melo, E.; Song, J.; Yue, S.; Piché, N.; Gauvin, R. Scanning Electron Microscopy versus Transmission Electron Microscopy for Material Characterization: A Comparative Study on High-Strength Steels. *Scanning* **2021**, *2021*, 1–19. https://doi.org/10.1155/2021/5511618.
(16) Toupin, M.; Bélanger, D. Thermal Stability Study of Aryl Modified Carbon Black by in Situ Generated Diazonium Salt. *J. Phys. Chem. C* **2007**, *111* (14), 5394–5401. https://doi.org/10.1021/jp066868e.